ONLINE FIRST

ISSN: 0015-5659

e-ISSN: 1644-3284

Evaluation of cell morphology and adhesion capacity of human gingival fibroblasts on titanium discs with different roughened surfaces: an in vitro scanning electron microscope analysis and cell culture study

Authors: H. Yildiz, E. Sen, H. Dalcik, S. E. Meseli

DOI: 10.5603/FM.a2022.0072

Article type: Original article

Submitted: 2022-07-08

Accepted: 2022-08-07

Published online: 2022-08-17

Evaluation of cell morphology and adhesion capacity of human gingival fibroblasts on titanium discs with different roughened surfaces: an *in vitro* scanning electron microscope analysis and cell culture study

H. Yildiz et al., Gingival fibroblast behaviors on titanium

H. Yildiz[1], E. Sen[2], H. Dalcik[3], S.E. Meseli[1]

[1]Istanbul Aydin University, Faculty of Dentistry, Periodontology Department, Istanbul, Turkey

[2]Istanbul Aydin University, Faculty of Medicine, Histology and Embryology Department, Istanbul, Turkey

[3]Istanbul Aydin University, Faculty of Medicine, Anatomy Department, Istanbul, Turkey

Address for correspondence: S.E. Meseli, Asst. Prof., Ph.D, DDS, Faculty of Dentistry, Periodontology Department, Istanbul Aydin University, Istanbul, Turkey, tel: +905304667471, fax: +902124255759, e-mail: suleymanmeseli@aydin.edu.tr

ABSTRACT

Background: Implantoplasty is an option in peri-implantitis treatment. What is known about the effects of implantoplasty on peri-implant soft tissue adhesion and cell behaviors is limited. This study aimed to evaluate the morphological features and adhesion capacity of human gingival fibroblast (HGF) cells onto sand-blasted, large-grit, acid-etched (SLA®) titanium (Ti) discs surfaces roughened with different implantoplasty protocols.

Materials and methods: The study included a total of 48 Ti discs divided into four groups (n=12) per group: Group I: machined, smooth surface discs; Group II: SLA® surface discs; Group III: SLA® surface discs roughened with diamond bur sequence (40 and 15-µm grit); Group IV: SLA® surface discs roughened with diamond bur sequence (125 and 40-µm grit). Following polishing procedure, the surface roughness value of

discs were assessed by a profilometer and scanning electron microscope (SEM). HGFs were cultured on Ti discs and cell adhesion was examined after the 24th, 48th, and 72nd hours. Statistical significance was set at the p≤0.05 level.

Results: SEM analyses of the discs revealed that fibroblasts exhibited well-dispersion and a firm attachment in all groups. The cells in group I and II had thin and long radial extensions from the areas where the nucleus was located to the periphery; however attached cells in group III and IV showed more spindle-shaped morphology. The surface roughness parameters of the test groups were lower than those of the SLA®. The SLA® group showed the highest HGF adhesion (group II) (p≤0.05). HGF adhesion in group IV was greater compared to group III, but less than group I.

Conclusions: This study showed that the characteristics of the burs applied in the implantoplasty protocol are determinant for the surface roughness and fibroblast adhesion occurs on surfaces with decrased roughness following implantoplasty. Consequently, it should be kept in mind that the surface properties of the implant may affect the adherent cell morphology and adhesion.

Key words: cell adhesion, cell morphology, human gingival fibroblasts, implantoplasty, surface roughness

INTRODUCTION

The peri-implant soft tissue surrounds the implant in the neck region like a tight collar. This structure, which is crucial for osseointegration of the implant, should adhere firmly to the implant surface [18]. The gingival epithelium proliferates along the implant surface without a connective tissue attachment due to the proximity of tissue fibers in parallel arrangement along the implant axis [16]. This fundamental phenomenon underlying the mechanism of soft tissue adaptation at the cellular level is still unknown.

Fibroblasts are the primary cells of the soft connective tissue of the periodontium. Inflammation of the periodontal tissue leads to a breakdown of fibroblasts and impaired tissue integrity. As a result of the progressive degenerative changes, a loss of periodontal tissue occurs. This pathogenesis, which manifests itself in periodontal tissues, is also observed in peri-implant tissues. The soft tissues surrounding the implant

function as a biological barrier and protect the peri-implant bone from microbiological infections [19].

HGFs exhibit a "filopodial" structure that extends further into grooves and microstructures on rough surfaces [7], which results in increased fibroblast adhesion [38]. On the contrary, HGFs accumulate more randomly on smooth surfaces [22]. Surface texture, such as roughness and topographical changes, influences connective tissue adhesion to the transmucosal section of implants. Various physical, chemical, and biochemical surface modification techniques were introduced to increase roughness and improve cell adhesion [3]. At the same time, these well-designed surface modifications must also minimize microbial colonization around the implant surface [17].

In vivo studies have shown a positive association between plaque accumulation rate and surface roughness in the supragingival region [9, 37]. To observe bacterial adherence and colonization in the oral cavity, where surface irregularities such as grooves, pits, perikymata, and abrasion defects are frequently present in scanning electron microscope (SEM) images [12]. Since it is difficult to remove microorganisms from these areas, they colonize and form biofilm structures. In the case of abutment materials with a rough surface, it was found that they contain twenty-five times more pathogenic bacteria than smooth materials [30]. In addition, smooth surfaces facilitate oral hygiene and improve fibroblast adhesion compared to roughened surfaces [41].

The roughness value (R_a) serves to determine the structural height of the surface and defines the arithmetic mean of the profile values [40]. In a subsequent investigation based on their previous short-term study [29], the researchers concluded that lowering the R_a value well below the 0.2 µm threshold had no significant effect on the gingival microbial colonization [5].

In the treatment of peri-implantitis, surgical treatments are required in addition to conventional treatment methods to ensure complete decontamination [5]. Implantoplasty, also known as mechanical modification of the implant, is recommended as part of surgical treatment to change implant surface topography, reduce microbial colonization, and thus prevent reinfection [1, 4, 32]. While it is not possible to completely eliminate microorganisms using current implantoplasty techniques, a

combination of mechanical and chemical techniques is more effective [35]. However, there are still experimental, non-standardized, and non-consensual implantoplasty techniques, so the mechanical or biological outcomes of these treatment approaches are still unknown.

The purpose of this *in vitro* study was to determine and compare the adhesion of HGF to*:* sand-blasted, large-grid, acid-etched (SLA®)- surfaced Ti discs after applying diamond bur sequences with different implantoplasty protocols. The null hypothesis of the present study was that surface modifications in implantoplasty procedures did not affect HGF growth and adhesion.

MATERIALS AND METHODS

Pre-made cell lines were used in the present 72-hour *in vitro* cell culture study. Therefore, approval from the ethics committee was not necessary.

Sample Size and Study Groups

Based on values from methodologically similar studies [22, 24, 25], the power analysis tool G-POWER calculated a total sample size of 48, with an effect size of 0.65, 95% power, and a margin of error of 0.56%. Groups were evenly distributed, with 12 discs in each group.

A total of 48 commercially available grade 4 pure titanium discs with a diameter of 10 mm and a thickness of 2.5 mm were used (Trias-ixx2, Servo Dental, Hagen, Germany). The discs met the biocompatibility requirements of the "Standard Specification for Unalloyed Titanium for Surgical Implant Applications" (ASTM F 67/ ISO 5832-2). Four groups each with 12 discs included in the study were:

- Group I: machined discs with smooth surfaces;
- Group II: SLA® discs with roughened surfaces;
- Group III: The SLA® discs were milled for two minutes with a round-tipped red diamond bur (40 μm grit, Dimei Royal, China); and for one-minute with a

round-tipped white diamond bur (15 µm grit, Komet Dental, Germany). Subsequently, all discs were polished with Brownie silicone under a one-minute water rinse;

- Group IV: SLA® discs were milled for two minutes with a round-tipped green diamond bur (125 µm grit, Dimei Royal, China); and for one-minute with a round-tipped white diamond bur (15 µm grit, Komet Dental; Germany). Subsequently, all discs were polished with Brownie silicone under a one-minute water rinse.

Standardization was maintained during the surface roughening protocol in groups III and IV with a custom-built stabilization mechanism. In a controlled environment, one of the researchers (HY) milled each disc clockwise from its center to its outer periphery for the specified time frame with a separate set of burs, while an external observer recorded the milling times for each disc. HY took a 5-minute break between each disc milling. This *in vitro* approach was used to model the milling process during implantoplasty [25]. As part of the preparation for cell culture, each disc was assigned a unique number. The R_a value of each disc was measured using a mechanical profilometer (MahrSurf M 400, Germany).

Cell Culture

Following *in vitro* milling procedures, all discs were agitated for 5 minutes in an ultrasonic cleaner and the samples were cleaned with 20% ethanol for 10 minutes. Discs were then autoclaved at 134 °C for 20 minutes under a gauge pressure of 2 kg/cm² (Dri-Tec, Canada).

The human gingival fibroblast cell line (HGF1; ATCC) was used for cell culture. Cells were passaged in flasks containing Dulbecco Modified Eagle Medium culturing media (HyClone, USA) containing 10% fetal bovine serum (Sigma-Aldrich Co., USA, the CAS number: 9014-81-7) and incubated at a temperature of 37 °C, relative humidity of 95% (to minimize media evaporation and condensation), and 5% CO_2. Upon reaching 80% confluency, the cells were then subcultured using with phosphate buffered saline (Sigma-Aldrich Co., USA, the CAS number: 7758-11-4) and a trypsin-

ethylenediaminetetraacetic acid solution (0.5 g/L trypsin; 0.2 g/L EDTA, Sigma-Aldrich Co., USA, the CAS number: 9002-07-7). Cells from passages 3 and 4 were used in this study.

Analysis of Cell Viability, Proliferation and Adhesion

To determine cell viability and proliferation, 3-(4,5-dimethylthiazol-2-yl)-2,5-diphenyltetrazolium bromide (MTT) (Sigma-Aldrich Co., USA, the CAS number: 57360-69-7) was used as the gold standard for assessing the metabolic activity of the cells. The sterilized discs of each group were placed in 24-well plates. Each well was seeded with 100.000 HGFs at a density of 100.000 cells/mL and incubated at 37 °C in a CO_2 incubator. The samples were transferred to a new 24-well plate after 24 hours. The wells were then filled with the MTT solution and placed in the incubator to determine cell viability and proliferation [25]. After 3.5 hours, a dimethyl sulfoxide (DMSO) solution (Sigma-Aldrich Co., USA, the CAS number: 67-68-5) was added to each well. Formazan products were transferred to a 96-well plate and the absorbance was measured at a reference wavelength of 570 nm. Cell proliferation and viability were measured after 24, 48, and 72 hours. The absorbance of formazan accepted that it was linearly correlated with the number of adhered cells and MTT-labeled cells are defined by their adhesion characteristics [6, 14, 27, 42].

Scanning Electron Microscope Analysis

A sample collection from each group was randomized using a computer-generated randomization table to assess surface topography, cell morphology and fibroblast adhesion by SEM (ZEISS EVO® LS 10, Yildiz Technical University, Turkey). Before the imaging, the samples were coated with a 10 nm thin gold layer.

Statistical Analysis

Statistical analysis of this study was performed using Statistical Package for Social Sciences version 24.00. The Kolmogorov-Smirnov test was used to assess the normality of the quantitative data. The Kruskal-Wallis test was used for multiple comparisons between groups, while the Mann-Whitney U test was used to compare the mean values

of two groups. Repeated measurements of the mean values of the groups were compared with Friedman's test. Existence of significant difference in repeated measurements, the mean values of the two groups were compared with Wilcoxon Signed Rank test. The level of statistical significance was set at $p \leq 0.05$.

RESULTS

The R_a values of the individual discs in each group are shown in Table I. The mean R_a value of group II ($p=0.001$) was found to be the highest, while group I ($p=0.001$) had the lowest value. There were also significant differences among the mean R_a values of the groups ($p \leq 0.05$).

The SEM analysis of each group showed that the surface topographies varied when the surfaces were treated with different burs. During the surface modification process, irregular structures, multiple grooves and protrusions formed on the SLA surfaces (Figures 1a, 1b, 1c, 1d). Due to the characteristics of the burs, mild surface irregularities occurred in groups III and IV.

SEM-generated morphologic micrographs showed that well-dispersed and evenly distributed cells that were firmly attached to the surfaces in all groups. The morphology of the cultured HGF were in close contact with each other and formed a carpet-like layer that adhered firmly to the Ti discs. The SEM images clearly showed the fibroblasts that exhibited thin and long radial extensions-marked with the arrows in the figures-from the cell nucleus zone to the periphery in groups I and II (Figures 2 and 3). But, considering the proliferation and adhesion areas revealed with the formazan crystals formed as the result of MTT assays, attached cells in group III and IV showed spindle-shaped morphology that the extensions of cells more closely located to nuclei (Figures 4 and 5).

For each study time point, there were significant differences between groups in terms of cell adhesion ($p=0.001$) (Table II). According to the pairwise comparisons, group III had the lowest adhesion rate ($p \leq 0.05$), while group II had the highest rate ($p \leq 0.05$). In addition, cell adhesion was significantly higher in group I than in group IV ($p \leq 0.05$).

When the mean cell adhesion values of the groups evaluated according to study time points, the significant difference was found only in group II ($p=0.035$). The mean percent cell adhesion values between groups showed that only the mean value of group II at 48 hours was significantly higher than that at 24 hours ($p=0.029$), while it was significantly lower at 72 hours ($p\leq0.05$) (Table II).

DISCUSSION

Several surface properties, including morphological properties, roughness, surface textures, and hydrophilicity, can affect cell adhesion and proliferation [26]. Ti surface modifications improve cell surface adhesion, cell migration, and bone apposition [23]. The goal of surface modifications in dental implants is to achieve a stable implant with enhanced soft tissue adaptation [23]. The adhesion behavior of fibroblasts is known to differ among materials with varying degrees of surface roughness. Although the rough surfaces of Ti materials may pose a greater challenge to the peri-implant tissue health, the soft tissue adaptation of these surfaces has been shown to improve significantly [28]. The study conducted by Keller et al. revealed that surface modifications have a significant effect on the surface characteristics of Ti surfaces as well as on biochemical responses and cell adhesion rates [34].

The results obtained from this *in vitro* study conducted without a bacterial model demonstrates that the adhesion potential of HGF is affected by the surface roughness of Ti. The maximum adhesion of the fibroblasts was observed in the SLA-surface group, which also had the highest surface roughness. Additionally, the findings in implantoplasty groups showed that adhesion rates of group III was less than that of group IV, as a consequence of the less surface roughness in group III. Considering all of them, the null hypothesis was rejected in this presented study.

Several studies evaluating implantoplasty protocols showed widely varying values for surface roughness. Ramel et al. found that the application of a short diamond sequence followed by silicone polishers or Arkansas stone sequences yielded in R_a values between 0.32 and 0.39 μm [20]. In another study, implantoplasty with diamond burs and silicone polishers on roughened surfaces resulted in R_a values of 4.0 μm [31]. Another study examined diamond, tungsten, and multilaminar burs without polishers and the

researchers found R_a values between 4.12 to 5.01 μm [36]. Maal et al. demonstrated that carbide burs achieve smoother surfaces than diamond burs [25]. They found that the surface roughness affects initial cell adhesion after implantoplasty and smoother surfaces enhanced fibroblast growth. Similar to previous studies, the present *in vitro* study without a bacterial environment showed that Ti discs with smooth surfaces had the lowest roughness values (group I) while the SLA discs had the highest values and the highest adhesion rates of gingival fibroblasts (group II). Depending on the properties of the dental burs, group IV had a higher roughness value than group III, suggesting that the adhesion properties of cultured HGFs to Ti discs with different surface morphologies could have significant implications on the milling approaches for implantoplasty.

The findings of an *in vitro* study concluded that a surface roughness of less than 0.2 μm can only be achieved by implementing chairside implantoplasty protocols [11]. Additionally, surface roughness can be reduced by polishing the surface with silicone burs after milling [10]. The mean R_a values in the implantoplasty groups were lower than those in the SLA group in our study; however, they were not close to the cut-off value of 0.2 μm. Despite extensive studies on the effects of surface roughness on the topography of the peri-implant mucosa, there are still conflicting results.
The results of animal model studies demonstrated that surface changes did not have a negative effect on the soft tissue interaction with implant surface [2, 13]. Furthermore, Cochran et al. found no differences in the probing depth of the peri-implant junction between implants surfaced with plasma sprayed and SLA [33]. On the contrary, human biopsy samples from acidified or oxidized junction areas of implants showed less epithelial downgrowth and longer connective tissues [8, 15]. However, in the current study, the maximum adhesion of the fibroblasts was observed in the SLA-surface group, which also had the highest surface roughness, indicating a positive association between surface roughness and fibroblast adhesion. Based on the data we collected, group III had lower adhesion levels compared to group IV. This finding is consistent with previous studies showing that fibroblasts respond differently to materials with different surface roughness values [25, 39]. Currently, these *in vitro* results without a bacterial environment cannot be directly translated into clinical applications due to the differences between *in vitro* and *in vivo* conditions. In this study, we experimentally

designed Ti surfaces with various surface properties. Intraoral Ti surfaces are rare due to their difficult nature, which is why the values of R_a were different from those measured *in vivo*.

To date, implantoplasty research has focused on surface roughness, surface coating, heat dissipation during operation, and fracture resistance [2, 25, 31, 36]. Another issue not addressed in this study was surface corrosion, which requires further investigation to determine its effectiveness. Soft tissue has been tightly adapted to the implant surface as a result of implantoplasty techniques. Ti residues released during implantoplasty may have detrimental effects on peri-implant tissues [21]. For this reason, implantoplasty should only be performed in situations where implants are supracrestally exposed or gingival recession as a result of peri-implant bone loss.

CONCLUSIONS

The surface roughness has a crucial role in fibroblast morphology and adhesion, however it is not the only factor affecting them. Therefore; the clinicians should not forget that the surface they create during implantoplasty should have a sufficient smoothness value to prevent microbial colonization and, at the same time, a sufficient roughness value to allow fibroblast adhesion. It should be considered that the present study has inherent limitations as an *in vitro* cell behavior study, and should be designed with different implantoplasty protocols. Our study emphasizes the importance of developing a standard implantoplasty protocol that does not compromise fibroblast adhesion while providing predictable outcomes.

Acknowledgement

The authors would like to acknowledge Servo Dental, Germany, for providing Ti discs and Bilim Implant, Turkey, for measuring the surface roughness values of the materials. We also thank M.Sc. Yusuf Iseri for the linguistic support he provided.

Funding

The authors declare that they have not received any financial support from any organizations, institutions, or individuals.

Conflict of interests

The authors declare that they have no current or potential conflict of interest related to this study.

REFERENCES

1. Albouy JP, Abrahamsson I, Perron LG, et al. Spontaneous progression of ligatured induced peri-impantitis at implants at implants with different surface characteristics. An experimental study in dogs II: histological observations. Clin Oral Implants Res 2009;20(4):366-371. https://doi.org/10.1111/j.1600-0501.2008.01645.x

2. Areid N, Willberg J, Kangasniemi I, et al. Organotypic in vitro block culture model to investigate tissue-implant interface. An experimental study on pig mandible. J Mater Sci Mater Med. 2021;32(11):136. https://doi.org/10.1007/s10856-021-06608-5

3. Bagno A, Di Bello C. Surface treatments and roughness properties of Ti-based biomaterials. J Mater Sci Mater Med 2004;15:935-949. https://doi.org/10.1023/b:jmsm.0000042679.28493.7f

4. Berglungh T, Gotfredsen K, Zitzmann NU, et al. Spontaneous progression of ligature induced peri-implantitis at implants with different surface roughness: an experimental study in dogs. Clin Oral Implants Res 2007 Oct;18(5):655-661. https://doi.org/10.1111/j.1600-0501.2007.01397.x

5. Bollen CML, Papaionnou W, Van Eldere J, et al. The influence of abutment surface on plaque accumulation and peri-implant mucositis. Clin Oral Implants Res 1996;7(3):201-211. https://doi.org/10.1034/j.1600-0501.1996.070302.x

6. Chen Y, Lu B, Yang Q, et al. Combined Integrin Phosphoproteomic Analysis and Small Interfering RNA-Based Functional Screening Identify Key Regulators for Cancer Cell Adhesion and Migration. Cancer Res 2009; 69(8):3713-3720. https://doi.org/10.1158/0008-5472.can-08-2515

7. Chou L, Firth JD, Uitto VJ, et al. Substratum surface topography alters cell shape and regulates fibronectin mRNA level, mRNA stability, secretion and assembly in human fibroblasts. J Cell Sci 1995;108:1563-1573. https://doi.org/10.1242/jcs.108.4.1563

8. Cochran DL, Buser D, ten Bruggenkate CM, et al. The use of reduced healing times on ITI implants with sandblasted and acid-etched (SLA) surface: early results from clinical trials on ITI SLA implants. Clin Oral Implants Res 2002;13:144-153. https://doi.org/10.1034/j.1600-0501.2002.130204.x

9. Conserva E, Generali L, Bandieri A, et al. Plaque accumulation on titanium disks with different surface treatments: an in vivo investigation. Odontology 2018 Apr;106(2):145-153. https://doi.org/10.1007/s10266-017-0317-2

10. Costa-Berenguer X, García-García M, Sánchez-Torres A, et al. Effect of implantoplasty on fracture resistance and surface roughness of standard diameter dental implants. Clin Oral Implants Res. 2018 Jan;29(1):46-54. https://doi.org/10.1111/clr.13037

11. de Souza Júnior JM, Oliveira de Souza JG, Pereira Neto AL, et al. Analysis of effectiveness of different rotational instruments in implantoplasty: An in vitro study. Implant Dent 2016;25(3):341-347. https://doi.org/10.1097/id.0000000000000381

12. Engel AS, Kranz HT, Schneider M, et al. Biofilm formation on different dental restorative materials in the oral cavity. BMC Oral Health 2020 Jun 3;20(1):162 https://doi.org/10.1186/s12903-020-01147-x

13. Englezos E, Cosyn J, Jacquet W, et al. Resective treatment of peri-implantitis: clinical and radiographic outcomes after 2 years. Int J Periodontics Restorative Dent 2018;38(5):729-35. https://doi.org/10.11607/prd.3386

14. Ghorbani FM, Kaffashi B, Shokrollahi P, et al. PCL/chitosan/Zn-doped nHA electrospun nanocomposite scaffold promotes adipose derived stem cells adhesion and proliferation, Carbohydr Poly 2015:118: 133-142. https://doi.org/10.1016/j.carbpol.2014.10.071

15. Glauser, Schüpbach P, Gottlow J, et al. Periimplant soft tissue barrier at experimental one-peace-mini-implants with different surface topography in humans: a light-microscope overview and histometric analysis. Clin Implant Dent Relat Res 2005;7(Supp. 1):S44-S51. https://doi.org/10.1111/j.1708-8208.2005.tb00074.x

16. Guy SC, McQuade MJ, Scheidt MJ, et al. In vitro attachment of human gingival fibroblasts to endosseous implant materials. J Periodontol 1993;64:542-546. https://doi.org/10.1902/jop.1993.64.6.542

17. Hayakawa T, Yoshinari M, Nemoto K, et al. Effect of surface roughness and calcium phosphate coating on the implant/bone response. Clin Oral Implants Res 2000;11:296-304. https://doi.org/10.1034/j.1600-0501.2000.011004296.x

18. Ivanovski S, Lee R. Comparison of peri-implant and periodontal marginal soft tissues in health and disease. Periodontol 2000 2018;76:116-130. https://doi.org/10.1111/prd.12150

19. Kawahara H, Kawahara D, Hashimoto K, et al. Morphological studies on the biological seal of titanium dental implants. Report I. In vitro study on the epithelization mechanism around the dental implants. Int J Oral Maxillofac Imp 1998;13;457-464.

20. Keller JC, Draughn RA, Wightman JP, et al. Characterization of sterilized CP titanium implant surfaces. Int J Oral Maxillofac Implants 1990;5:360-367.

21. Kim H, Murakami H, Chehroudi B, et al. Effects of surface topography on the connective tissue attachment to subcutaneous implants. Int J Oral Maxillofac Implants 2006;21:354-365.

22. Lee SW, Kim SY, Rhyu IC, et al. Influence of microgroove dimension on cell behaviour of human gingival fibroblasts cultured on titanium substrata. Clin Oral Implants Res 2008;20:56-66. https://doi.org/10.1111/j.1600-0501.2008.01597.x

23. Lim YJ, Oshida Y, Andres CJ, et al. Surface characterizations of variously treated titanium materials. Int J Oral Maxillofac Implants 2001;16:333-342.

24. Louropoulou A, Slot DE, Van der Weijden FA. Titanium surface alterations following the use of different mechanical instruments: a systemic review. Clin Oral Implants Res 2012;23:643-658. https://doi.org/10.1111/j.1600-0501.2011.02208.x

25. Maal M B, Ellingsen SA, Reseland J E, et al. Experimental implantoplasty outcomes correlate with fibroblast growth in vitro. BMC Oral Health 2020;20-25. https://doi.org/10.1186/s12903-020-1012-

26. Martinez MAF, Balderrama IF, Karam PSB, et al. Surface roughness of titanium disks influences the adhesion, proliferation and differentiation of osteogenic properties derived from human. Int J Implant Dent 2020;6;46. https://doi.org/10.1186%2Fs40729-020-00243-5

27. Miki I, Ishihara N, Otoshi M, et al. Simple colorimetric cell-cell adhesion assay using MTT-stained leukemia cells. J Immunol Methods, 1993;164:255-261. https://doi.org/10.1016/0022-1759(93)90318-2

28. Ong JL, Prince CW, Raikar GN, et al. Effect of surface topography of titanium on surface chemistry and cellular response. Implant Dent 1996;5(2):83-88.

29. Quirynen M, Bollen CM, Papaioannou W, et al. The influence of titanium abutment surface roughness on plaque accumulation and gingivitis: short-term observations. Int J Oral Maxillofac Implants. 1996;11(2):169-178.

30. Quirynen M, Van der Mei H, Bollen CML, et al. An in vivo study of the influence of roughness of implants on the microbiology of supra and subgingival plaque. J Dent Res 1993;72:1304-1309. https://doi.org/10.1177/00220345930720090801

31. Ramel CF, Lüssi A, Özcan M, et al. Surface roughness of dental implants and treatment time using six different implantoplasty procedures. Clin Oral Implants Res 2016;25:776-781. https://doi.org/10.1111/clr.12682

32. Renvert S, Persson GR, Pirih FQ, et al. Peri-implant health, peri-implant mucositis, and peri-implantitis: Case definitions and diagnostic considerations. J Clin Periodontol 2018;45 Suppl 20:S278-S285. https://doi.org/10.1186/s12903-020-1012-1

33. Schwarz F, Ferrari D, Herten M, et al. Effects of surface hydrophilicity and microtopography on early stages of the soft tissue integration at non-submerged titanium implants: an immunohistochemical study in dogs. J Periodontol 2007;78:2171-2184. https://doi.org/10.1902/jop.2007.070157

34. Sculean A, Gruber R, Bosshardt DD. Soft tissue wound healing around teeth and dental implants. J Clin Periodontol 2014;41:6-22. https://doi.org/10.1111/jcpe.12206

35. Stavropoulos A, Wikesjo UM. Growth and differentiation factors for periodontal regeneration: a review on factors with clinical testing. J Periodontal Res 2012;47:545-553. https://doi.org/10.1111/j.1600-0765.2012.01478.x

36. Tawse-Smith A, Kota A, Jayaweera Y, et al. The effect of standardised implantoplasty protocol on titanium surface roughness: an in-vitro study. Braz Oral Res 2016 Dec 22;30:e137. https://doi.org/10.1590/1807-3107bor-2016.vol30.0137

37. Teranaka A, Tomiyama K, Ohashi K, et al. Relevance of surface characteristics in the adhesiveness of polymicrobial biofilms to crown restoration materials. J Oral Sci 2018 Mar 24;60(1):129-136. https://doi.org/10.2334/josnusd.16-0758

38. Walboomers XF, Monaghan W, Curtis ASG, et al. Attachment of fibroblasts on smooth and microgrooved polystyrene. J Biomed Mater Res 1999;46:212-220. https://doi.org/10.1002/(sici)1097-4636(199908)46:2%3C212::aid-jbm10%3E3.0.co;2-y

39. Watzak G, Zechner W, Tangl S, et al. Soft tissue around three different implant types after 1.5 years of functional loading without oral hygiene: a preliminary study in baboons. Clin Oral Implants Res 2006;17:229-236. https://doi.org/10.1111/j.1600-0501.2005.01217.x

40. Wennerberg A, Albrektsson T. Effects of titanium surface topography on bone integration: a systematic review. Clin Oral Implants Res 2009;20:172-178. https://doi.org/10.1111/j.1600-0501.2009.01775.x

41. Zhang F, Huang Y, Li X, et al. Surface modification and its effect on attachment, spreading, and proliferation of human gingival fibroblasts. Int J Oral Maxillofac Implants 2011;26:1183-1192.

42. Zheng S, Guan Y, Yu H, et al. Poly-l-lysine-coated PLGA/poly (amino acid)-modified hydroxyapatite porous scaffolds as efficient tissue engineering scaffolds for cell adhesion, proliferation, and differentiation. New J Chem 2019:43;9989-10002.

Table I. Discs R_a values

Discs	Group I	Group II	Group III	Group IV
1	0.317	1.099	0.577	1.057
2	0.224	1.418	0.757	0.824
3	0.221	1.360	0.889	1.098
4	0.196	1.532	0.449	0.897
5	0.439	1.087	0.582	0.914
6	0.145	1.093	0.614	0.752
7	0.165	0.908	0.456	0.728
8	0.263	1.538	0.731	0.740
9	0.127	1.282	0.511	0.817
10	0.258	1.480	0.506	0.743
11	0.162	1.712	0.501	0.947
12	0.320	1.714	0.655	0.834
Mean ± Sd	0.236±0.09	1.351±0.26	0.602±0.13	0.862±0.12

n: Number, Mean±Sd: Mean±Standard deviation

Table II. Inter- and intra-group comparisons of fibroblast adhesion

	Standard	**Group I**	**Group II**	**Group III**	**Group IV**	
	Mean±Sd (%) Min-Max (Median) (%)	Mean±Sd (%) Min-Max (Median) (%)	Mean±Sd (%) Min-Max (Median) (%)	Mean±Sd (%) Min-Max (Median) (%)	Mean±Sd (%) Min-Max (Median) (%)	***p**
24th hours	100±0.25 99.75-100.32 (99.96)	60.83±0.73$^{\text{œ}}$ 60-61.54 (60.89)	66.48±0.39$^{\Delta, \S}$ 66.04-66.84 (66.52)	35.58±1.61$^{¥}$ 33.37-37.15 (35.89)	51.78±0.74 51.23-52.87 (51.5)	***0,001***
48th hours	100±1.57 98.64-101.58 (99.88)	61.14±2.23$^{\text{œ}}$ 58.58-63.52 (61.24)	69.54±1.83$^{\Delta, \mu}$ 67.61-71.86 (69.26)	36.25±2.22$^{¥}$ 33.35-38.2 (36.73)	52.61±0.55 51.97-53.24 (52.61)	***0,001***
72nd hours	100±5.95 96.08-108.82 (97.54)	63.5±1.38$^{\text{œ}}$ 62.14-65.24 (63.31)	72.94±5.54$^{\Delta}$ 66.81-80.24 (72.27)	35.91±2.45$^{¥}$ 32.3-37.48 (36.93)	54.87±6.37 50.93-64.36 (52.1)	***0,001***
¶p	0.397	0.077	**0.035**	0.668	0.437	-

%: Percentage, Mean±Sd: Mean±Standard deviation, Min.-Max: Minimum-maximum,

p<0.05: *Kruskal-Wallis Test; Mann-Whitney U Test $^{\Delta}$(Group II – I/III/IV) $^{¥}$(Group III-I/IV) $^{\text{œ}}$(Group I-IV),

p<0.05: ¶Friedman Test; Wilcoxon Signed Rank Test §(24th hour-48th hour/72nd hour)$^{\mu}$(48th hour-72nd hour).

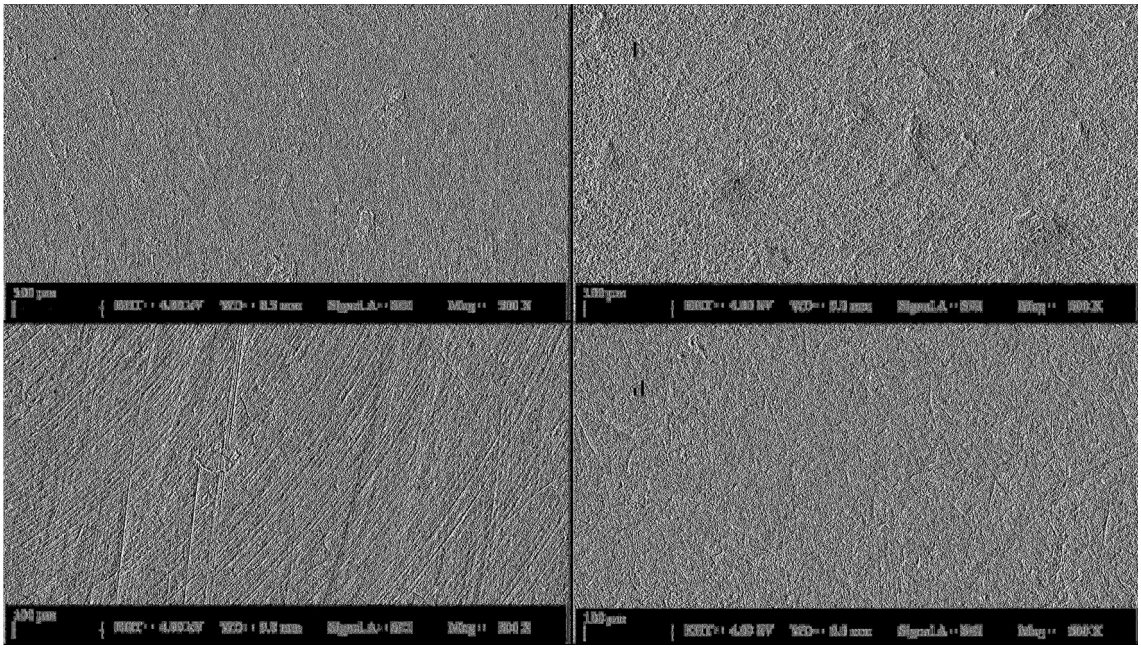

Figure 1: SEM images of surface topographies of the Ti discs (500X magnification); **a:** Group I, **b:** Group II, **c:** Group III, **d:** Group IV

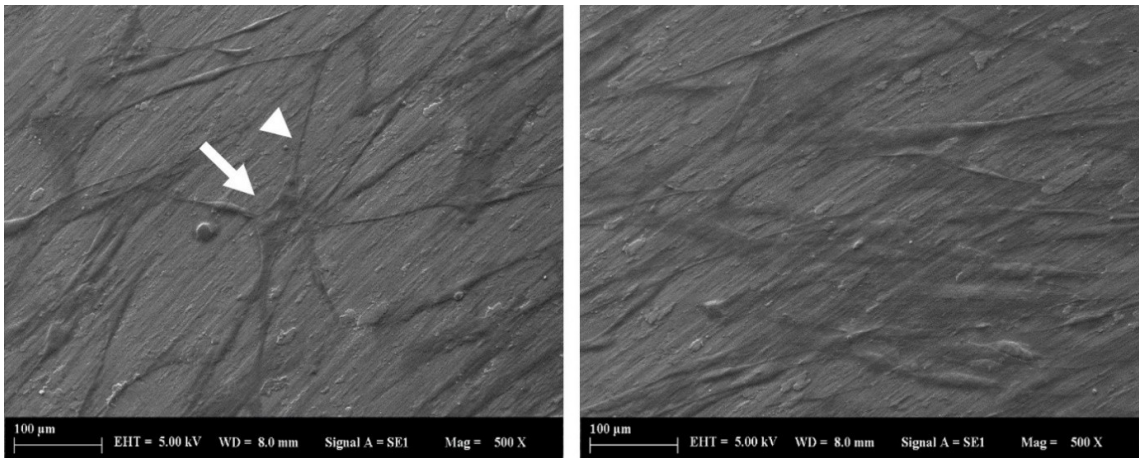

Figure 2: SEM images of fibroblast Group I (24th hour, 500X magnification) (**Arrow:** Cell body; **Arrow Head:** Cytoplasmic extension)

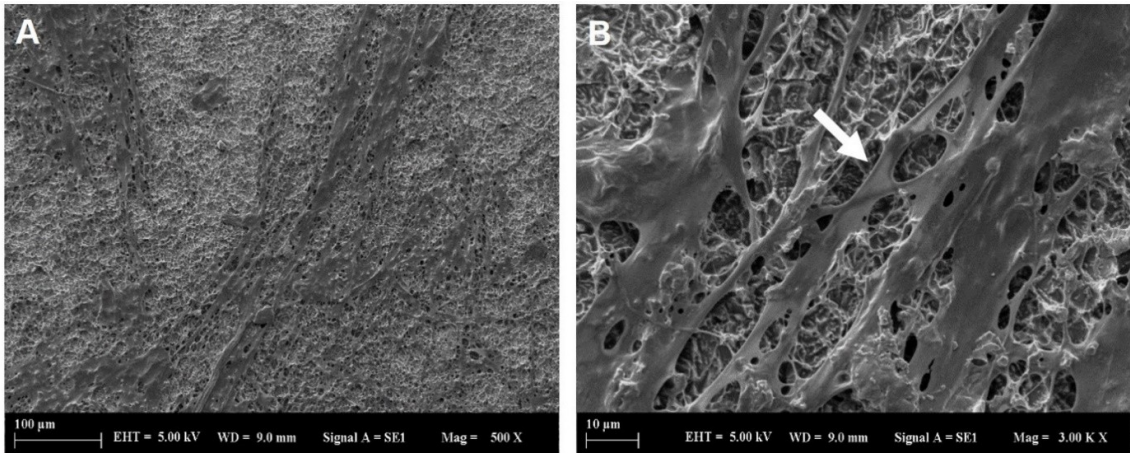

Figure 3: SEM images of fibroblast Group II (24th hour, A:500X, B:3000X magnification) (**Arrow:** Cytoplasmic extension)

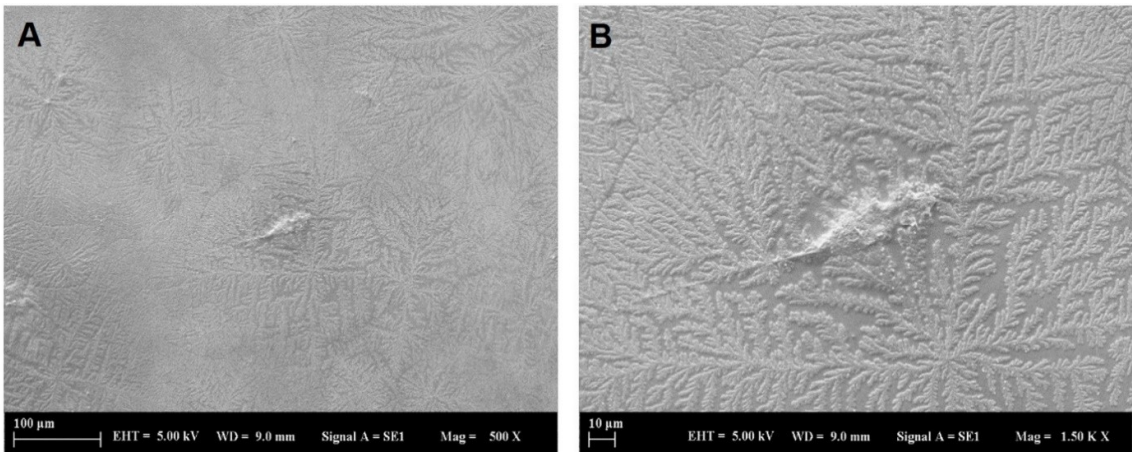

Figure 4: SEM images of cellular cytoplasmic adhesion areas in Group III (24th hour, A: 500X, B: 1500X magnification)

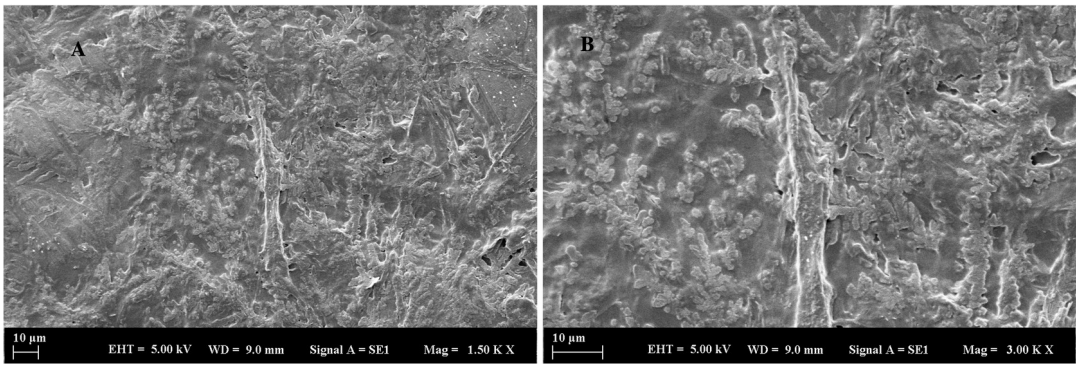

Figure 5: SEM images of fibroblast Group IV (24th hour, A:1500X, B:3000X magnification)